ANTIOXIDANTS & REDOX SIGNALING
Volume 20, Number 1, 2014

DOI: 10.1089/ars.2012.4752

ORIGINAL RESEARCH COMMUNICATION

Ceramide Mediates Acute Oxygen Sensing in Vascular Tissues

Laura Moreno,[1–3] Javier Moral-Sanz,[1–3] Daniel Morales-Cano,[1–3] Bianca Barreira,[1–3] Enrique Moreno,[1–3] Alessia Ferrarini,[4] Rachele Pandolfi,[1–3] Francisco J. Ruperez,[4] Julio Cortijo,[2,5,6] Manuel Sanchez-Luna,[7] Eduardo Villamor,[8] Francisco Perez-Vizcaino,[1–3] and Angel Cogolludo[1–3]

Abstract

Aims: A variety of vessels, such as resistance pulmonary arteries (PA) and fetoplacental arteries and the ductus arteriosus (DA) are specialized in sensing and responding to changes in oxygen tension. Despite opposite stimuli, normoxic DA contraction and hypoxic fetoplacental and PA vasoconstriction share some mechanistic features. Activation of neutral sphingomyelinase (nSMase) and subsequent ceramide production has been involved in hypoxic pulmonary vasoconstriction (HPV). Herein we aimed to study the possible role of nSMase-derived ceramide as a common factor in the acute oxygen-sensing function of specialized vascular tissues. ***Results:*** The nSMase inhibitor GW4869 and an anticeramide antibody reduced the hypoxic vasoconstriction in chicken PA and chorioallantoic arteries (CA) and the normoxic contraction of chicken DA. Incubation with interference RNA targeted to *SMPD3* also inhibited HPV. Moreover, ceramide and reactive oxygen species production were increased by hypoxia in PA and by normoxia in DA. Either bacterial sphingomyelinase or ceramide mimicked the contractile responses of hypoxia in PA and CA and those of normoxia in the DA. Furthermore, ceramide inhibited voltage-gated potassium currents present in smooth muscle cells from PA and DA. Finally, the role of nSMase in acute oxygen sensing was also observed in human PA and DA. ***Innovation:*** These data provide evidence for the proposal that nSMase-derived ceramide is a critical player in acute oxygen-sensing in specialized vascular tissues. ***Conclusion:*** Our results indicate that an increase in ceramide generation is involved in the vasoconstrictor responses induced by two opposite stimuli, such as hypoxia (in PA and CA) and normoxia (in DA). *Antioxid. Redox Signal.* 20, 1–14.

Introduction

Some specialized cells are able to respond rapidly to changes in oxygen tension within the physiological range in a manner that contributes to maintenance of oxygen homeostasis in the whole body (55). These include glomus cells of the carotid body, neuroepithelial bodies in the lungs, chromaffin cells of the fetal adrenal medulla, and specialized vascular smooth muscle cells present in resistance pulmonary arteries (PA), fetoplacental arteries, and ductus arteriosus (DA). Resistance PA and fetoplacental arteries contract in response to moderate hypoxia, while the increase in oxygen causes contraction of the DA (55).

Hypoxic pulmonary vasoconstriction (HPV) allows shifting blood flow from hypoxic to normoxic lung areas, thereby coupling ventilation and perfusion (55). HPV is considered to be responsible for the high pulmonary vascular resistance during fetal life. A similar mechanism for flow matching has been proposed in the fetoplacental vasculature, so that hypoxic vasoconstriction of fetoplacental arteries would divert

[1]Department of Pharmacology, School of Medicine, Universidad Complutense Madrid, Madrid, Spain.
[2]Centro de Investigaciones Biomédicas en Red de Enfermedades Respiratorias (CIBERES), Bunyola, Spain.
[3]Instituto de Investigación Sanitaria Clínico San Carlos (IdISSC), Madrid, Spain.
[4]Center for Metabolomics and Bioanalysis (CEMBIO), Facultad de Farmacia, Universidad CEU San Pablo, Madrid, Spain.
[5]Department of Pharmacology, School of Medicine, University of Valencia, Valencia, Spain.
[6]Fundación Investigación, Hospital General Universitario de Valencia, Valencia, Spain.
[7]Servicio de Neonatología, Hospital General Universitario Gregorio Marañón, Madrid, Spain.
[8]Department of Paediatrics, School for Oncology and Developmental Biology (GROW), Maastricht University Medical Centre (MUMC+), Maastricht, The Netherlands.

Innovation

Some vessels are specialized in detecting and responding to acute changes in oxygen tension. The results from the present study are consistent with a prominent role of neutral sphingomyelinase (nSMase)-derived ceramide in the hypoxic contraction in pulmonary arteries and chorioallantoic arteries and in the normoxic contraction of the ductus arteriosus. These data provide evidence for the proposal that nSMase-derived ceramide is a unifying mediator of acute oxygen-sensing in specialized vascular tissues.

blood flow to the placental areas with better maternal perfusion (21, 23, 25, 55). On the other hand, the increase in oxygen tension at birth is a key factor stimulating DA constriction, which precedes the permanent closure of the vessel (45, 55). Therefore, oxygen sensing in PA, fetoplacental arteries and DA play crucial roles during fetal life and in the transition to postnatal life.

Elucidation of the mechanisms involved in acute oxygen sensing in vascular smooth muscle cells has been the matter of intensive effort. It is now generally accepted that the physiological responses to changes in oxygen requires the existence of an oxygen sensor coupled to a signal transduction system, which in turn activates a variety of effector mechanisms (46, 52, 54). Intriguingly, despite opposite stimuli, hypoxic contraction of PA and fetoplacental arteries and normoxic contraction of the DA appear to share common mechanistic features. For instance, voltage-gated potassium (Kv) channels are inhibited by hypoxia in PA (2, 8, 56) and in fetoplacental arteries (20) and by normoxia in DA (34, 47), which suggest that these oxygen-sensitive K^+ channels constitute a conserved effector mechanism in these cells. The inhibition of Kv channels likely contributes to depolarization of the cell membrane and subsequent activation of voltage-gated L-type calcium channels and, accordingly, calcium channel blockers inhibit the hypoxic vasoconstriction in PA (8, 32, 53) and fetoplacental arteries (25) and the normoxic DA contraction (11, 33). In addition, other common mechanisms for HPV and normoxic DA contraction have been reported, such as release of calcium from intracellular stores (24, 27, 37), voltage-independent calcium entry (22, 26) and increase in Rho kinase activity (22, 26, 43).

The chicken embryo is a suitable model for studying developmental vascular biology (13). As compared to other models, the responses to normoxia in the DA (1, 7) and to hypoxia in PA (58) and chorioallantoic arteries (CA), the avian homologue of human fetoplacental arteries, (28) are consistent, robust, and reproducible in the chicken. Moreover, they do not require an agonist-induced pretone which preclude the possible influence of a preconstriction agent on the intracellular signaling mediating the responses to oxygen changes. Interestingly, in the chicken DA, the pulmonary and the aortic parts of the vessel can be morphologically and functionally distinguished. Thus, the pulmonary side (pDA) is a muscular artery which responds to normoxia with contraction, while the aortic side (aDA) is an elastic artery, which responds to normoxia with relaxation (1, 4, 7). This offers an excellent opportunity to comparatively search for an exclusive oxygen-sensitive mechanism in different portions of the same vessel.

Ceramide can be generated in cells *via de novo* biosynthesis pathway involving serine palmitoyl transferase or be synthesized from membrane sphingomyelin by sphingomyelinases (SMase), which are activated by multiple membrane receptors and nonreceptor stimuli (18). We have previously found that neutral SMase (nSMase)-derived ceramide acts as a critical mediator in the HPV response in rats by increasing reactive oxygen species (ROS) production *via* NADPH oxidase (8, 14). However, the possible role of ceramide in other oxygen-sensing tissues remains to be explored. Here we show that two opposite stimuli, such as hypoxia (in PA and CA) and normoxia (in pDA) increase ceramide production to promote vasoconstriction in chicken vessels. Moreover, inhibition of nSMase also prevented the HPV and oxygen-induced DA contraction in human tissues.

Results

Hypoxic contraction is reduced by nSMase inhibition in PA and CA

In chicken PA incubated under normoxic conditions, exposition to hypoxia led to a triphasic (contraction–relaxation–contraction) response. The second contraction reached a plateau after 10–12 min (Fig. 1A). To ascertain the role of nSMase in HPV, a second challenge to hypoxia was elicited in the absence (vehicle) or in the presence of an anticeramide antibody (15B4) or the nSMase inhibitor GW4869. Both treatments inhibited the contraction induced by hypoxia in PA (Fig. 1A, B), the inhibitory effects of GW4869 being concentration-dependent (12.5%±5.7%, 25.7%±5.1%, and 56.3%±7.2% for 0.1, 1, and 10 μM). Moreover, downregulation of nSMAse by siRNA also almost fully inhibited HPV (Fig. 1C, D) but had no effect on the contractile response to exogenous addition of bacterial SMase (Fig. 1D). CA responded with a transient contraction during the 10-min exposure to hypoxia (Fig. 1E). Similar to HPV, the hypoxic CA contraction was reproducible and inhibited by GW4869 (Fig. 1E, F). Unlike the hypoxic responses, the contractions induced by endothelin-1 (ET-1, 30 nM) were not affected by GW4869 in either PA or CA (Fig. 1G).

Normoxic contraction of the DA is reduced by nSMase inhibition

Exposure to normoxia in chicken pDA caused a reproducible contraction, which was inhibited by the anticeramide antibody and the nSMase inhibitor (Fig. 2A, B). Again the contraction induced by ET-1 in the DA was not affected by GW4869 (Fig. 2C). In another set of experiments, the normoxic contraction was tested in the presence of a PKCζ peptide inhibitor (PKCζ-PI, 10 μM) or Gö6976 (0.1 μM) an inhibitor of classic and novel protein kinase C (PKC) isoforms but without effect on the atypical isoform PKCζ. PKCζ-PI reduced the normoxic contraction of the DA, while Gö6976 was without effect (Fig. 2D).

Increase in ceramide content by hypoxia in PA and by normoxia in DA

In freshly isolated PA smooth muscles cells (PASMC) incubated in normoxic conditions, exposure to hypoxia for 10 min led to a marked increase in ceramide content measured by the fluorescence of permeabilized cells immunostained with an anticeramide antibody (Fig. 3A). DA smooth muscle cells (DASMC) isolated from the pDA or the aDA were incubated in hypoxia and exposed to normoxia for 10 min. Interestingly, normoxia markedly increased ceramide content

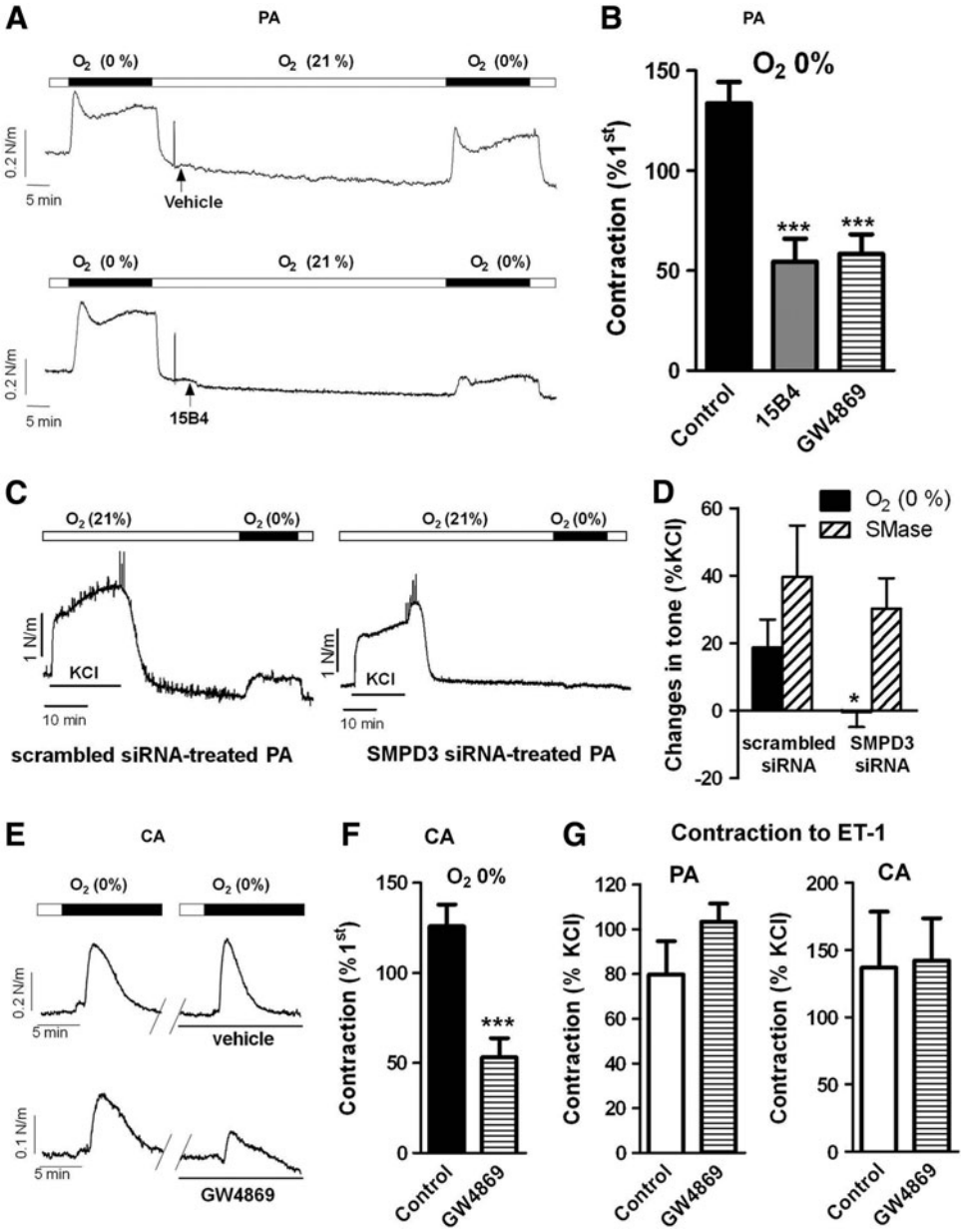

FIG. 1. Hypoxic contractions in chicken PA and CA are attenuated by nSMase inhibition. Representative traces **(A)** and average values **(B)** of HPV in the absence (vehicle) or the presence of the anticeramide antibody 15B4 (200 ng/ml) or the nSMase inhibitor GW4869 (10 μM). Representative traces **(C)** and average values **(D)** of HPV in *SMPD3*-targeted siRNA treated PA *versus* scrambled siRNAs-treated PA. The responses to exogenous SMase (100 mU/ml) are also shown in **(D)**. Representative traces **(E)** and average values **(F)** of the hypoxic response in CA in the absence (vehicle) or the presence of GW4869. **(G)** Shows the lack of effect of GW4869 on the contraction induced by ET-1 (30 nM) in PA and CA. In PA, hypoxic response was measured at the end of the exposure, while in CA the maximal response was analyzed. Data are expressed as a percentage of an initial response to hypoxia or to KCl. Results are means ± SEM. * and *** indicate $p < 0.0.5$ and $p < 0.001$ *versus* control ($n = 4$–8). PA, pulmonary arteries; CA, chorioallantoic arteries; nSMase, neutral sphingomyelinase; HPV, hypoxic pulmonary vasoconstriction; ET-1, endothelin-1.

in smooth muscle cells isolated from pDA but not in those isolated from aDA (Fig. 3B). In Figure 3C, the confocal images of nonpermeabilized PASMC show that ceramide can be exposed at the extracellular surface and bound by the anticeramide antibody. The increased in ceramide content after hypoxia in PA was further confirmed using ultra high performance liquid chromatography–mass spectrometry (UHPLC-MS). Figure 3D shows that hypoxia increased significantly the most abundant ceramide (d18:1/16:0) and a similar trend was observed for the other ceramides. A marked increase in this ceramide was also found in PA after exposure with bacterial SMase for 10 min, which served as a positive control (0.08 ± 0.008 *vs.* 5.8 ± 3.8 ceramide/phosphatidylcholine [PC]) in control and SMase-treated PA, respectively; $n = 5$; $p < 0.05$). Moreover, in PASMC exposed to hypoxia, ceramide levels recovered after 10 min of re-exposure to normoxia.

Increase in ROS production by hypoxia in PA and by normoxia in DA

We have previously reported that the contraction of rat PA in response to acute hypoxia and ceramide is associated with NADPH oxidase-mediated ROS generation (14). Likewise, hypoxia increased ROS production in chicken PA as determined by 2,7-dichlorofluorescein (DCF) fluorescence (Fig. 4A) and this increase was inhibited by the NADPH oxidase inhibitor VAS2870. The inset in Figure 4A shows that hypoxia-induced ROS increase was reversible after returning to normoxia. In the pDA, exposure to normoxia also led to an increase in ROS production (Fig. 4B). When the pDA were incubated with the NADPH oxidase inhibitor apocynin (300 μM), showed a decrease in ROS levels upon the normoxic challenge (Fig. 4B). Furthermore, incubation with apocynin or with the more selective inhibitor VAS2870 similarly reduced

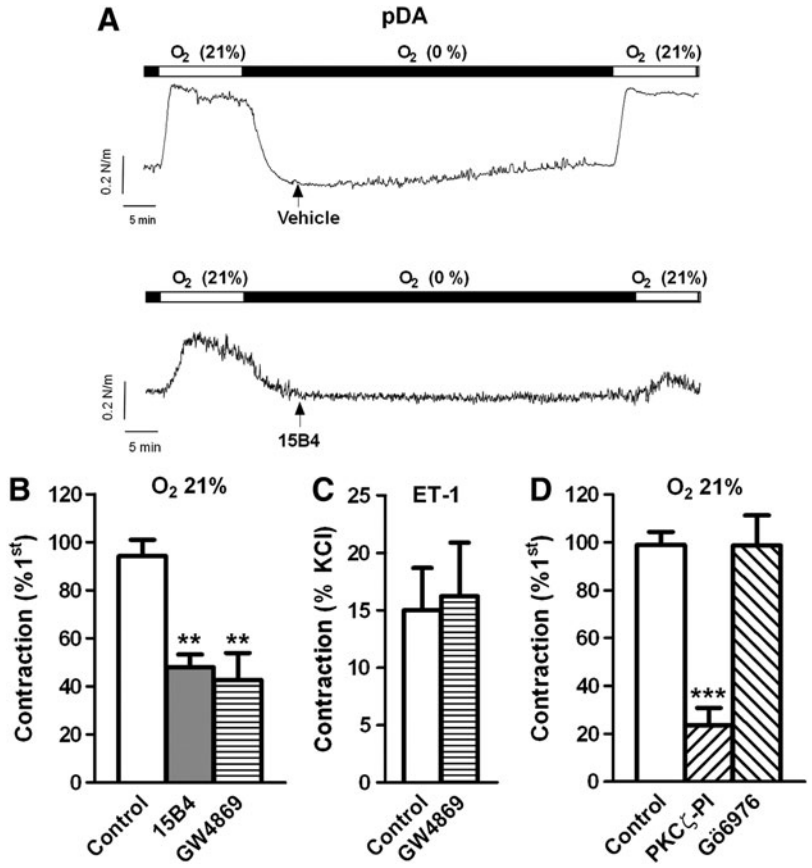

FIG. 2. The normoxic contraction of the pDA is attenuated by nSMase inhibitors. Representative traces **(A)** and average values **(B)** of the contraction induced by normoxia in the absence (control) or the presence of the anticeramide antibody 15B4 (200 ng/ml) or the nSMase inhibitor GW4869 (10 μM). Data are expressed as a percentage of an initial response to normoxia. Normoxic contraction was measured at the end of the exposure. **(C)** Shows the lack of effect of GW4869 on the contraction induced by ET-1 (30 nM). **(D)** Effects of PKCζ-PI (10 μM) and the classic PKC inhibitor Gö6976 (0.1 μM) on the contraction induced by normoxia. Results are means ± SEM. ** and *** indicate $p < 0.01$ and $p < 0.001$, respectively, *versus* control ($n = 4$–11). pDA, pulmonary side of the ductus arteriosus; PKC, protein kinase C; PKCζ-PI, PKCζ peptide inhibitor.

the hypoxic vasoconstriction in PA (Fig. 4C) and the normoxic contraction of the pDA (Fig. 4D). In addition, HPV response was markedly impaired by the presence of the mitochondrial electron transport chain inhibitors rotenone (complex I, 30 μM) and myxothiaxol (complex III, 10 μM) as compared to parallel controls (23% ± 12%, 16% ± 10%, and 148% ± 22% of the first hypoxic response, respectively). Likewise, rotenone inhibited hypoxia-induced ROS increase in PA (25% ± 4% and −11% ± 15% in control *vs.* rotenone-treated PA; $p < 0.05$).

Expression of SMPD3

As compared to PA and pDA, aDA was relatively insensitive to changes in oxygen in terms of ceramide production, which could reflect changes in the expression of nSMase. To test this possibility, mRNA levels of nSMase in pDA, aDA, PA, and CA were quantified. Quantitative real-time–polymerase chain reaction (RT-PCR) analysis revealed a reduced expression in aDA as compared to PA. No significant differences were found between aDA and pDA (Fig. 5).

Endogenous and exogenous ceramide mimic the effects of hypoxia in PA and CA, and the effects of normoxia in the DA

In another set of experiments, vessels were exposed to C_6-ceramide (10 or 30 μM) or to SMase from *Bacillus cereus* (100 mU/ml), that cleaves membrane sphingomyelin and release endogenous ceramide. Addition of C_6-ceramide or SMase contracted PA and CA (Fig. 6A), mimicking the effects of acute hypoxia (Fig. 6B). C_6-ceramide and SMase also contracted pDA, while relaxed aDA (Fig. 6C), mimicking the responses to normoxia in pDA and aDA (Fig. 6D). In addition, the incubation with the PKCζ-PI (10 μM) reduced the contraction of the pDA induced by C6-ceramide (2.2% ± 5.2% of KCl-contraction, $n = 6$; $p < 0.05$ *vs.* control).

Ceramide inhibits Kv currents in PA and pDA

In agreement with previous studies in rat PASMC, exposure to ceramide (Fig. 7A, B) or to acute hypoxia (Fig. 7B) inhibited Kv currents in chicken PASMC. The inhibitory effects of hypoxia and ceramide were comparable to those elicited by the Kv channels blocker 4-aminopyridine. Interestingly, ceramide also inhibited the potassium current present in pDASMC (Fig. 7C), mimicking the effects of 4-aminopyridine and normoxia (Fig. 7D) in these cells.

Effects of GW4869 in human vessels

Finally, we tested the effects of GW4869 in HPV and in the normoxic DA contraction in human tissues. The drug inhibited both the normoxic contraction of the DA (Fig. 8A, B) and the hypoxic contraction of the PA (Fig. 8C). Moreover, exogenous addition of ceramide (10 μM) also contracted human DA (22% ± 5% of the normoxic response, $n = 4$).

Discussion

In the present article, we show that ceramide is involved in acute vascular oxygen sensing. Pharmacological and genetic inhibition of the ceramide-generating enzyme nSMase

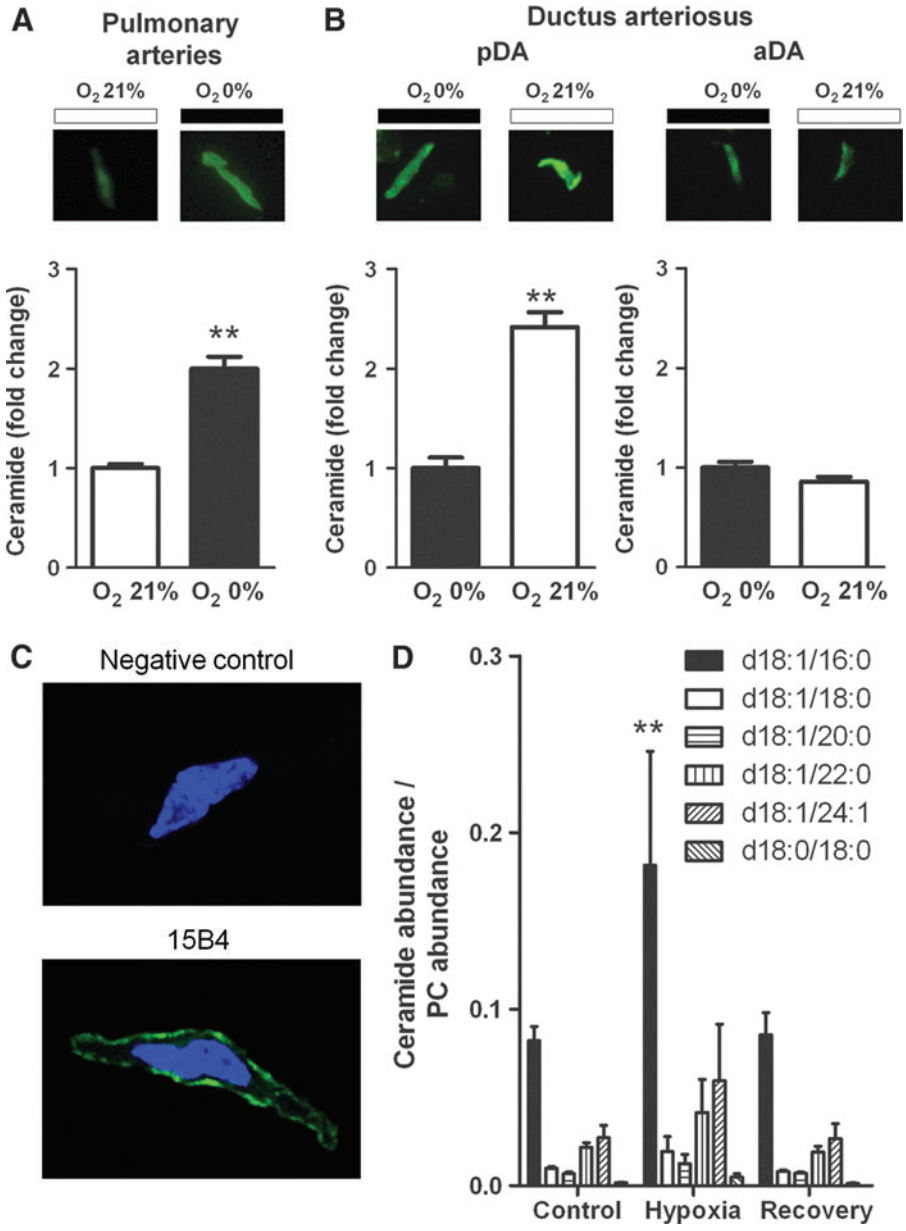

FIG. 3. Increase in ceramide production by hypoxia in PA and by normoxia in pDA. (A, B) Representative pictures (*top panels*) and average values (*bottom panels*) of ceramide content in cells isolated from **(A)** PA, **(B)** pDA or aDA exposed to normoxia or hypoxia and immunostained with a monoclonal ceramide-specific antibody (15B4). Results are means ± SEM of the averaged FITC-fluorescence intensity relative to cell surface measured in at least 90 cells present in 3–4 coverslips, each derived from a different animal. ** indicates $p < 0.01$ normoxia *versus* hypoxia (unpaired *t*-test). **(C)** Representative picture taken in a confocal microscope of a nonpermeabilized isolated cell exposed to hypoxia and immunostained with anticeramide antibody (15B4) and its negative control (without primary antibody). **(D)** Levels of different ceramides measured by UHPLC-MS in arteries exposed to normoxia (control), to 10 min hypoxia or to 10 min hypoxia followed by 10 min to normoxia (recovery). Data were normalized by the most abundant membrane lipid phosphatidylcholine 34:2 (PC). ** Bonferroni test after two way ANOVA. aDA, aortic side of the ductus arteriosus. To see this illustration in color, the reader is referred to the web version of this article at www.liebertpub.com/ars

reduced the hypoxic vasoconstriction in PA and CA and the normoxic contraction of the DA. Moreover, ceramide content and ROS production were increased by hypoxia in PA and by normoxia in DA. Accordingly, ceramide mimicked the contractile responses of hypoxia in PA and CA and those of normoxia in the DA. In addition, ceramide inhibited Kv currents present in PASMC and DASMC. Finally, the role of nSMase in acute oxygen sensing was confirmed in human PA and DA.

Hypoxic PA contraction

HPV allows shifting blood flow from hypoxic to normoxic lung areas, thereby coupling ventilation and perfusion (46, 49). Despite intensive effort, the precise mechanisms involved in HPV have not been fully clarified. While there is general consensus that the oxygen sensor resides in the mitochondria (46, 49, 52, 54), a variety of effector mechanisms have been reported to play a role in HPV, including calcium release from intracellular stores, closure of Kv channels, opening of voltage-gated calcium channels and nonselective cation channels and calcium sensitization *via* Rho kinase activation (2, 30, 43, 44, 46). However, the most contentious area concerns the signaling mechanisms that link the mitochondrial sensor to the effectors. Thus, some authors propose that ROS decrease during hypoxia, while others propose that ROS increase during hypoxia (49, 51, 54). In previous studies, we have shown that acute hypoxia increases ROS in rat PA through an integrated signaling pathway, which includes activation of nSMase, increase in ceramide production and PKCζ-dependent NADPH oxidase activation (8, 14). Our results showing a NADPH-dependent Kv channel inhibition by hypoxia (8, 14) have been more recently confirmed by Mittal *et al.* (35). Herein we show that acute hypoxia also increases ceramide and ROS production in chicken PASMC. Moreover, the nSMase inhibitor GW4869, the siRNA against *SMPD3* (the gene

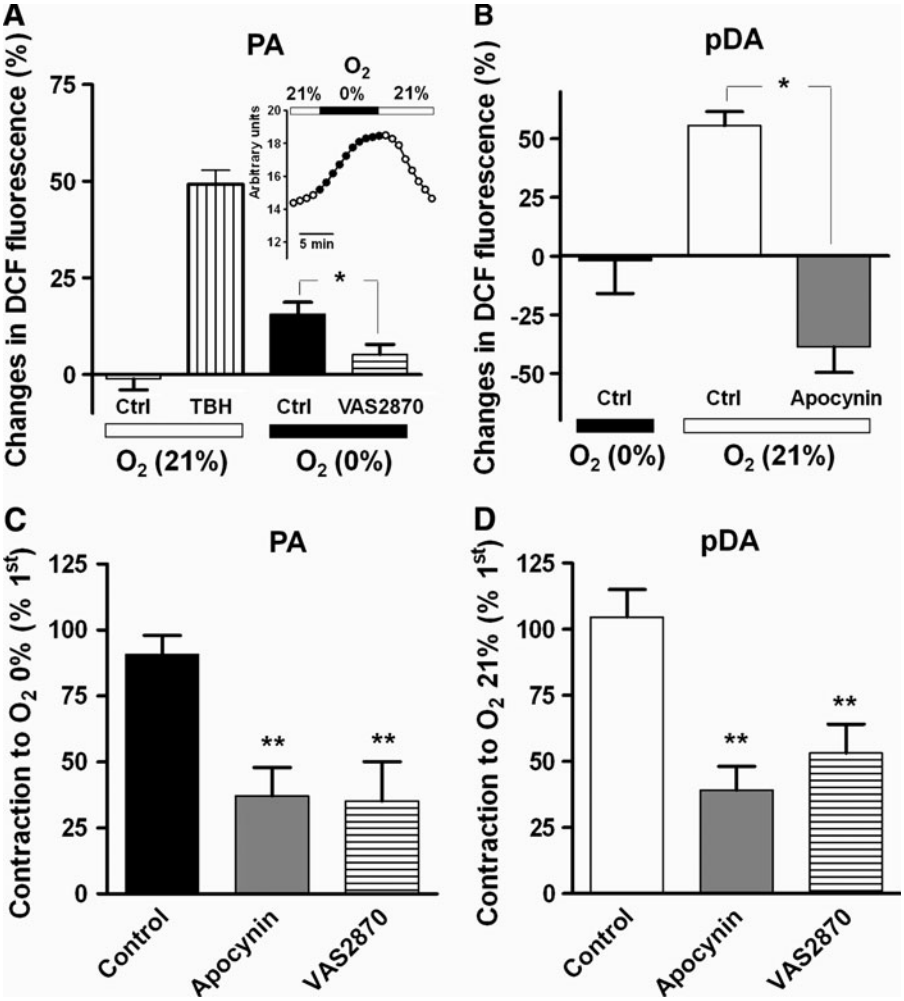

FIG. 4. ROS production and its role in the contractile responses. (A) ROS production (measured by the green fluorescent of DCF-DA) induced by hypoxia in PA and its inhibition by the NAPDH oxidase inhibitor VAS2870 (30 μM). Parallel experiments were performed under 21% O_2 in the absence (time control) or in the presence of TBH (positive control). A representative experiment of the time course of ROS increase induced by hypoxia and the reversal after normoxia was re-established is shown in inset. **(B)** ROS production induced by normoxia in pDA and its inhibition by apocynin (300 μM). **(C, D)** Inhibitory effects of apocynin and VAS2870 in PA **(C)** and pDA **(D)**. Results are means ± SEM. ** indicates $p < 0.01$ *versus* control ($n = 4$–8). ROS, reactive oxygen species; DCF, 2,7-dichlorofluorescein; TBH, t-butylhydroperoxide.

encoding nSMase2), and the NADPH oxidase inhibitors apocynin and VAS2870 reduced HPV in chicken PA. GW4869 also inhibited HPV in human PA, which suggest that this mechanism of oxygen sensing is widely present in vertebrates. HPV was also inhibited by the anticeramide-antibody which reflects that ceramide may be exposed in the outer leaflet of the plasma membrane since antibodies are not able to cross the membrane. This was confirmed by immunocytochemistry in nonpermeabilized cells. Although it is generally believed that ceramides in the plasma membrane are segregated into rigid domains or rafts, they may be rapidly transferred across the membrane to the outer leaflet and vice versa flip-flop (3, 12, 31). Thus, ceramide generated as a second messenger may recruit its signaling targets (*e.g.*, PKCζ) to the inner surface of the membrane (19) but also be exposed to the extracellular surface.

Hypoxic CA contraction

It has been proposed that, similar to HPV, hypoxic fetoplacental vasoconstriction would divert fetal blood flow toward regions receiving better maternal perfusion (20, 23, 55). Moreover, resembling HPV, inhibition of Kv channels has been reported to contribute to hypoxic fetoplacental vasoconstriction (20). The avian homologous of mammalian fetoplacental arteries are CA which perfuse the late embryonic organ for gas-exchange, the chorioallantoic membrane. Like human fetoplacental vessels (20), chicken CA constrict in response to acute hypoxia (28). Herein we show that the hypoxic contraction of CA is decreased after nSMase inhibition. In agreement with previous reports, our observations argue in favor of a common mechanism for hypoxic vasoconstriction in PA and fetoplacental arteries.

Normoxic DA contraction

At birth, closure of the DA is crucial for the adaptation from fetal to postnatal life. In full term, infants the increase in oxygen tension at birth leads to DA constriction which precedes the anatomical and permanent closure of the vessel (45, 55). Thus, the DA behaves exactly opposite to PA and CA, since it contracts during normoxia and relaxes to hypoxia. Paradoxically, the effector mechanisms responsible for HPV and the normoxic contraction of the DA seem to be virtually the same. These include: Kv channel inhibition (33), Rho kinase activation (22, 26), activation of store operated calcium entry encoded by transient receptor potential cation channels channels (22) and calcium release from intracellular stores (27). In contrast with the discrepancies reported in the HPV field, most evidences support a role of increased ROS in the normoxic DA contraction (55). As mentioned for the PA, the reported mechanisms for oxygen sensing/signaling are

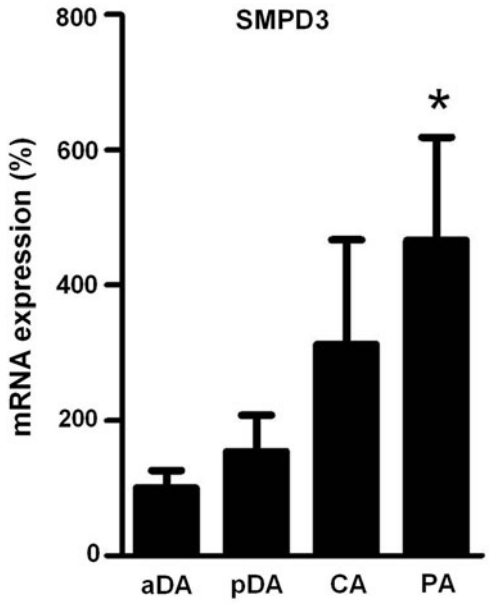

FIG. 5. *SMPD3* expression in chicken pDA, aDA, PA, and CA. Expression of the nSMase2 gene *SMPD3* analyzed by real-time–polymerase chain reaction. Results are normalized to GAPDH and expressed as a percent of mean values of aDA. Results are means ± SEM ($n = 3$–6). * indicates $p < 0.05$ PA *versus* aDA (one-way ANOVA followed by a Bonferroni's test).

similar in mammalian and chicken DA (7, 17). In the present study we show that, similar to HPV, the normoxic contraction of the pDA was attenuated by nSMase and NADPH oxidase inhibitors. Furthermore, oxygen increased ceramide production in SMC isolated from pDA but not in those from aDA, the portion of the vessel that lacks a normoxic contraction (1, 11). In rat PA, we have found that hypoxia-induced $p47^{phox}$ phosphorylation and ROS production were prevented by inhibition of nSMase or PKCζ (14), a well known target of ceramide (5, 36, 40). Likewise, contraction of pDA induced by normoxia and ceramide were reduced by a PKCζ inhibitor.

One potential limitation of our study was the use of the same hypoxic and normoxic conditions for all vessels studied. Our hypoxic conditions yielded pO_2 values of ~3 kPa, comparable to those estimated to occur in the fetal PA and DA (15). However, our normoxic conditions (~18 kPa), representative of normoxic ventilation, may approach those detected in PA (46, 48), but exceed the pO2 values that the DA sense after the newborn starts breathing.

Ceramide mimics the effects of changes in oxygen concentration

In our previous study, we showed that nSMase2 mRNA expression was ~10-fold higher in PA compared to mesenteric arteries (8). Thus, the specific increase in ceramide production observed in oxygen sensing in vascular cells could reflect differences at the level of nSMase expression. Herein we found a trend for higher expression in the mRNA expression of *SMPD3* in PA, pDA, and CA as compared to aDA,

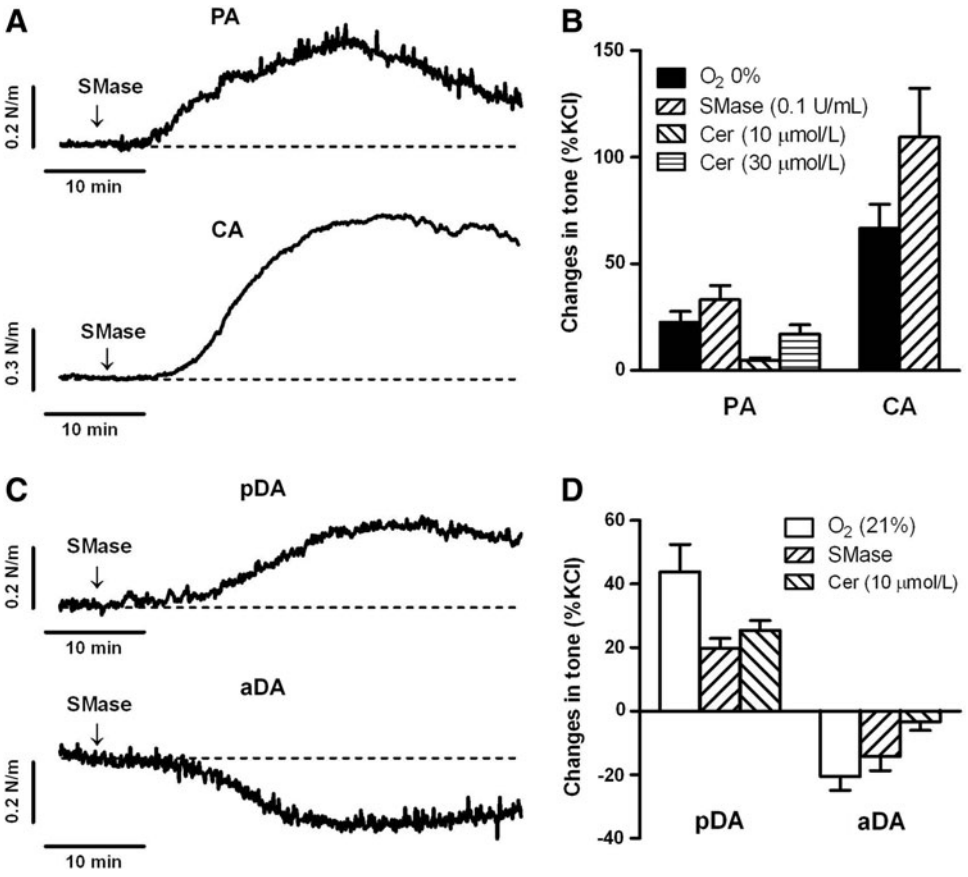

FIG. 6. Exogenous addition of bacterial SMase and ceramide reproduces the effects of hypoxia in PA and CA and the effects of normoxia in pDA and aDA. Representative traces **(A, C)** and average values **(B, D)** of the contractile responses induced by SMase (100 mU/ml from *Bacillus cereus*) or C_6-ceramide (10 or 30 μM) in PA, CA, pDA, and aDA. The effects of hypoxia (in PA and CA) and normoxia (pDA and DA) are also included for comparison purposes. Vascular responses were expressed as a percentage of an initial response to KCl (60 m*M*). Results are means ± SEM ($n = 5$–12).

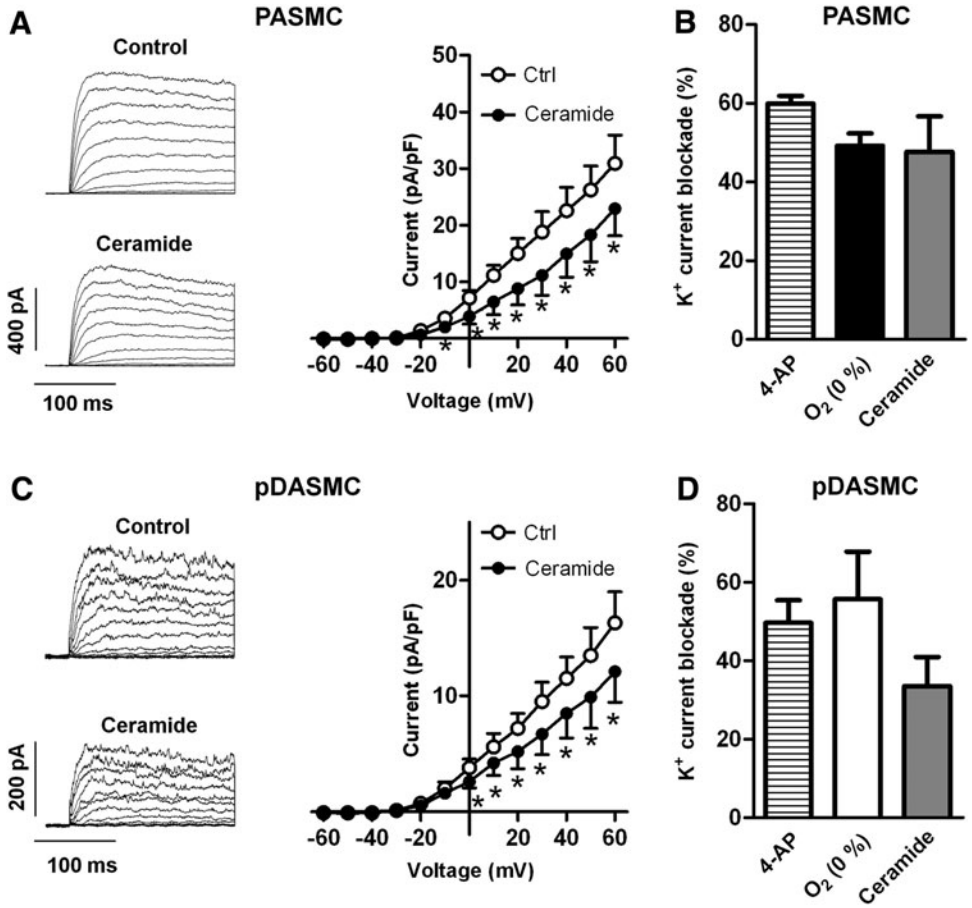

FIG. 7. Ceramide inhibits Kv currents in PASMC and DASMC. (A, C) Representative current traces for 200-ms depolarization pulses from −60 mV to +60 mV in 10 mV increments from a holding potential −60 mV before (control) and after 10 μM C_6-ceramide in PASMC **(A)** or pDASMC **(C)**. *Right panels* show the current–voltage relationships of Kv currents measured at the end of the pulse before (control) and after the addition of C_6-ceramide ($n = 6$). **(B)** K^+ current blockade induced by 4-AP (1 mM), hypoxia and C_6-ceramide at +60 mV in PASMC. **(D)** K^+ current blockade induced by 4-AP, normoxia and C_6-ceramide at +60 mV. Results are means ± SEM. * indicates $p < 0.05$ *versus* control (paired Student's *t*-test). Kv, voltage-gated potassium; PASMC, pulmonary artery smooth muscle cell; DASMC, ductus arteriosus smooth muscle cells; 4-AP, 4-aminopyridine.

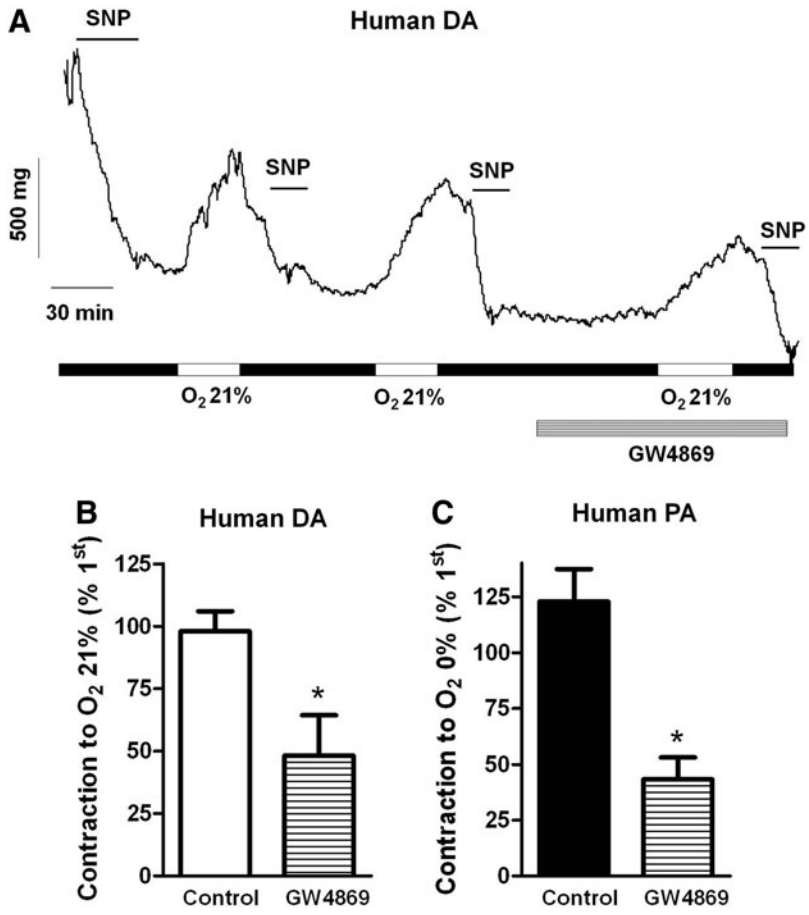

FIG. 8. GW4869 inhibits hypoxic PA contraction and normoxic DA contraction in human vessels. (A) Original experiment showing the contractile responses induced by repetitive exposures to normoxia in a human DA. The last exposure was performed in the presence of GW4869. SNP (10 μM) was used as indicated to accelerate the otherwise slow and incomplete relaxation. **(B, C)** Average values of the contractions induced by normoxia in human DA and by hypoxia in human PA in the absence or in the presence of the nSMase inhibitor GW4869 (10 μM). Data are expressed as a percentage an initial response to normoxia or hypoxia in the absence of the drug. * indicates $p < 0.05$ *versus* control. Results are means ± SEM ($n = 3$–5). SNP, sodium nitroprusside.

although only the former reached statistical significance. Unfortunately, we could not study possible differences at the protein level due to the lack of commercial antibodies for chicken nSMase2. Therefore, the specific responses observed in oxygen sensing cells may be partly attributable to differences nSMase expression. In a striking similarity with the effects of changes in oxygen tension, addition of SMase and ceramide contracted PA, CA, and pDA, while relaxed aDA. These effects resemble those induced by hydrogen peroxide which inhibits the oxygen-sensitive Kv currents and causes contraction of the PA (14) and the pDA (7), while relaxes the aDA. These results support the notion that oxygen sensitive responses require not only ceramide production but also the presence of exclusive oxygen-sensitive effector mechanisms targeted by ceramide.

Kv channel modulation

Despite the functional contribution of Kv channels in HPV, it is still a matter of controversy, it is generally accepted their modulation by changes in oxygen tension. Therefore, we focus on Kv channels as well recognized oxygen sensing effectors in PA (2, 56), DA (34, 47), and fetoplacental arteries (20). Accordingly, Kv channels were inhibited by hypoxia in chicken PA (present study) and by normoxia in pDA (7). In addition, ceramide inhibited Kv currents present in SMC from chicken PA and pDA, again mimicking the effects of these opposite stimuli. Interestingly, the nature of the Kv channel subunits most likely to generate the oxygen-sensitive Kv current in both PASMC and DASMC appears the same (*i.e.*, Kv1.5 and Kv2.1) (55). It has been proposed that hypoxia decreases Kv current by shifting the PASMCs to a more reduced redox status, while the inhibition of Kv currents induced by normoxia in the DASMC results from a more oxidized environment (34, 53). In agreement with this idea, reducing and oxidizing agents (at relatively high concentrations) mimic the effects of hypoxia in PA and normoxia in DA, respectively (38). A still unanswered question in this model is how a more reduced redox status in the PA and an oxidized environment in the DA lead to the inhibition of virtually the same Kv channels. Moreover, the reducing agent GSH inhibits not only the hypoxic-sensitive Kv currents in PASMC but also the hypoxic-insensitive Kv currents in mesenteric arteries (57). Alternatively, we propose that inhibition of Kv channels by opposite stimuli involves a common mediator (*i.e.,* ceramide and ROS). In agreement with our proposal, not only ceramide (present study) but also t-butylhydroperoxide (at concentrations in the micromolar range), inhibit Kv currents and cause vasoconstriction in both PA and DA (7, 14, 42). Moreover, inhibition of endogenous H_2O_2 production by increasing intracellular catalase through the patch pipette prevented the inhibition of Kv currents induced by hypoxia in PA and by normoxia in DA (7, 14, 42). Another argument in favor of our proposal arises from the fact that ceramide inhibits the hypoxic-sensitive Kv currents in PASMC but not the hypoxic-insensitive Kv currents in mesenteric arteries (36).

Therefore, based on this and previous reports (8, 11, 14, 36) we propose a common signaling pathway for oxygen sensitive vessels involving the activation of nSMase. The ceramide generated *via* activation of PKCζ leads to NADPH-derived ROS production. Among other targets, ROS inhibit Kv channels and lead to vessel contraction.

Unresolved issues

Although the identity of the oxygen sensor remains unknown, substantial body of evidence supports the concept that mitochondria acts as the oxygen sensor in specialized oxygen sensing tissues (46, 52, 54). In agreement with this idea, hypoxic contraction in rat (14) and chicken (present study) PA and the normoxic contraction of the DA (7, 17) are blunted by inhibitors of complex I and III of the mitochondrial electron transport chain. Moreover, the complex I inhibitor rotenone prevents hypoxia-induced ceramide and ROS production in rat (14) and chicken (present study) PA. However, the mechanisms matching the sensor to nSMase remain unknown. Intriguingly, nSMase is a redox-sensitive enzyme that can be activated by an increase in ROS (18, 29). Thus, one possibility is that in both situations, hypoxia in PA and normoxia in DA, nSMase is activated by mitochondrial-derived ROS. It is conceivable that normoxia increases mitochondrial ROS generation in the DA by providing more oxygen as substrate. Likewise, hypoxia is able to increase mitochondrial-derived ROS in PA and probably in systemic arteries (52). Therefore, activation of nSMase, production of ceramide and subsequent NADPH oxidase-derived ROS might represent an amplification pathway downstream the sensor (14, 39, 41) present only in specialized oxygen sensing cells.

A number of nonvascular cells, such as the glomus cells of the carotid body, neuroepithelial bodies in the lungs or chromaffin cells of the fetal adrenal medulla are also able to acutely respond to changes in oxygen tension. The results from the present study raise the question of whether nSMase-derived ceramide might also participate in oxygen sensing in these tissues. However, it has been reported that the response to hypoxia in the carotid body is not affected by the nSMase inhibitor GW4869 (16). The possible role of ceramide in other oxygen sensing tissues warrants future studies.

Materials and Methods

Animal experiments were performed in accordance with the Spanish legislation and the procedures were approved by the review board of the Complutense University of Madrid. The Human Studies Committee of Hospital Gregorio Marañón and Hospital General Universitario de Valencia approved the use, after informed consent, of discarded DAs and lung tissue, respectively, excised during surgery. DAs derived from five neonates with hypoplastic left heart syndrome ($n=3$) or coartaction of the aorta ($n=2$), while lung tissue was obtained from three adult patients with lung carcinoma surgery.

Reagents

Unless stated otherwise, drugs and reagents were obtained from Sigma-Aldrich Quimica. Ethanol (HPLC-grade) and ammonium (Reagent-grade) were purchased from Panreac Quimica, formic acid (98%) and LC-MS grade methanol were purchased from Fluka Analytical. The mouse anticeramide 15B4 antibody was from Alexis (Grupo Taper). Drugs were dissolved in distilled water except C_6-ceramide, GW4869 and rotenone in DMSO and myxothiazol in ethanol. Final vehicle concentrations were $\leq 0.1\%$.

Egg incubation and tissue isolation

Fertilized eggs of White Leghorn chickens were incubated at 38°C, and automatically rotated once per hour (Brinsea Polyhatch incubator). Embryos were incubated for 19–20 days of the 21-day incubation period or allowed to hatch, and then transferred to a brooder chick box (Novital Brooder Chick Box, PY333) for up to 3 days. During the grow-out period, chickens were provided *ad libitum* access to water and a standard starter diet. Animals were euthanized by decapitation, and the DA, the chorioallantoic membrane, or the lungs were removed and immersed in ice-cold Krebs buffer (composition in m*M*: NaCl 118, KCl 4.75, $NaHCO_3$ 25, $MgSO_4$ 1.2, $CaCl_2$ 2.0, KH_2PO_4 1.2 and glucose 11). Right and left DA and CA were sampled at 19–20 days of incubation (noninternally pipped embryos), while PA were isolated from 2- to 3-day-old chickens.

Vessel and cell isolation

Vessels were isolated as previously described (1, 11, 28, 58). Briefly, secondary branches of the PA and tertiary branches of the CA were carefully dissected free of surrounding tissue and cut into rings (1.8–2 mm length). The DAs were divided in two segments referred to as pulmonary and aortic DA (pDA and aDA, respectively).

PASMC and DASMC were isolated by enzymatic digestion as previously described (10, 11). For cell isolation, endothelium-denuded vessels were dissected into a physiological salt solution (PSS) of composition (in m*M*): NaCl 130, KCl 5, $MgCl_2$ 1.2, $CaCl_2$ 1.5, glucose 10, HEPES 10 (pH 7.3 with NaOH). PA rings were incubated in a Ca^{2+}-free PSS containing (in mg/ml) papain 1, dithiothreitol 0.8 and albumin 0.7 for 5–7 min. DA rings were initially incubated at 4°C in Ca^{2+}-free PSS containing elastase I (0.28 mg/ml) for 5 min. Thereafter, DA was incubated at 37°C in a low Ca^{2+} (10 μM) PSS containing collagenase I (1 mg/ml), collagenase XI (1 mg/ml), papain (0.15 mg/ml), and ditiothreitol (1.5 mg/ml) for additional 5 min. After enzymatic incubation, tissues were washed in Ca^{2+}-free PSS and disaggregated using a wide bore, smooth-tipped pipette. Cells were stored in Ca^{2+}-free PSS (4°C) and used within 8 h (7, 10). To maintain a hypoxic environment, solutions for DASMC digestion and storage contained the oxygen scavenger sodium dithionite (0.8×10^{-3} M; pH adjusted to 7.4 with NaOH) (7, 10).

Normoxia and hypoxia

For contractile tension recording, the chambers were filled with Krebs buffer maintained at 37°C. To achieve normoxic conditions, solutions were continuously aerated with 21% O_2–5% CO_2–74% N_2 (pO2 = 17–19 kPa). Hypoxia was induced by gassing the chamber with 95% N_2/5% CO_2 (pO_2 = 2.6–3.3 kPa). For the other *in vitro* experiments, cells and isolated vessels were placed in a chamber of 0.5 ml and perfused with a normoxic (oxygen in equilibrium with room air) or a hypoxic PSS at a rate of 2 ml/min. In these experiments, hypoxia was achieved by vigorously bubbling the PSS solution with 100% N_2 in a film coated reservoir. This led to an oxygen concentration of 3%–4% in the chamber as measured with an oxygen Clarck electrode (WPI Instruments).

Recording of arterial reactivity

Contractile responses in endothelium-intact PA, CA, and DA rings mounted in a wire myograph were recorded as previously reported (1, 11, 36). Human DA rings (internal diameter 3–5 mm) were mounted in conventional organ baths. PA and CA were mounted under normoxic condition; while DA rings were maintained under hypoxic conditions (see above). After an equilibration period of 30 min, chicken vessels and human resistance PA (internal diameter 300–400 μm) were distended to a resting tension corresponding to a transmural pressure of 2.66 kPa, while human DA were mounted between two hooks under a tension of 30 mN. Preparations were firstly stimulated by raising the K^+ concentration of the buffer (to 80 m*M*) in exchange for Na^+. Vessels were washed three times and allowed to recover before a new stimulation.

In preliminary experiments, we ascertained that vessels were able to respond to successive challenges to hypoxia (for PA and CA) or normoxia (for DA) in the absence of a preconstrictor agent. Therefore, each vessel was exposed to two hypoxic (PA and CA) or normoxic (DA) challenges. The second challenge was examined after 1 h incubation with vehicle (control), anticeramide antibody (15B4, 200 ng/ml), the nSMase inhibitor GW4869 (10 μM), the classic PKC inhibitor Gö6976 (0.1 μM), PKCζ-PI (0.1 μM), the NADPH oxidases inhibitors apocynin (300 μM), and VAS2870 (30 μmol) or the mitochondrial electron transport chain inhibitors rotenone (complex I, 30 μM) and myxothiaxol (complex III, 10 μM) and the contractile responses were expressed as a percentage of the first challenge. In some experiments, the effects of C_6-ceramide (10 μM), SMase from *B. cereus* (100 mU/ml) or ET-1 (30 n*M*) were tested in the absence and the presence of GW4869. The contractile responses induced by these agents were expressed as a percentage of the initial response to KCl.

Human DA showed and intrinsic contractile tone that was not reversed upon continuous wash-out with hypoxic Krebs solution. Therefore, to study oxygen-induced contractions all human DA rings were initially relaxed by sodium nitroprusside (SNP, 100 μM). Thereafter, DAs were washed three times with drug free Krebs solution. After 40 min equilibration rings were challenged to normoxia. Similar procedure was used before subsequent exposures to normoxia.

Introduction of siRNA by reverse permeabilization

Reverse permeabilization was used to introduce siRNA into isolated chicken PA (6). Briefly, PA were exposed to three successive solutions (4°C) containing (in m*M*) (i) 10 EGTA, 120 KCl, 5 Na_2ATP, 2 $MgCl_2$, 20 HEPES and 50 n*M* siRNA (pH 6.8; 30 min); (ii) 120 KCl, 5 Na_2ATP, 2 $MgCl_2$, and 20 HEPES and 50 n*M* siRNA (pH 6.8; 180 min); and (iii) 120 KCl, 5 Na_2ATP, 10 $MgCl_2$, and 20 HEPES and 50 n*M* siRNA (pH 6.8; 30 min). Subsequently, PA were bathed in a fourth solution containing (in m*M*) 120 NaCl, 5 KCl, 5 Na_2ATP, 10 $MgCl_2$, 5.6 glucose, and 10 HEPES (pH 7.1, 4°C), in which $[Ca^{2+}]$ was gradually increased from 0.001 to 0.01 to 0.1 to 1 m*M* every 15 min. Vessels were then placed in DMEM culture medium supplemented with L-glutamine (2 m*M*), penicillin (100 U/ml), and streptomycin (100 μg/ml) and maintained in an incubator (37°C, 95% O_2/5% CO_2) for 3 days before assessing vascular contractility.

A mixture of four siRNAs (including one Cy3-labelled siRNA) targeting different regions of chicken nSMase was

used. After 24 h incubation, some vessels were examined using fluorescence microscopy to assess siRNA uptake. In preliminary studies, siRNA efficiency was measured by RT-PCR confirming a reduction in *SMPD3* mRNA levels by 51% ± 12% at 72 h, as compared to vessels exposed to random siRNA (scramble).

Immunofluorescent detection of ceramide content

Freshly isolated PASMC or DASMC were allowed to settle on gelatine-coated coverslips for 20 min. PASMC were initially perfused with normoxic PSS for 25 min and thereafter, some coverslips were kept in normoxia and others changed to hypoxic PSS during the last 5 min. On the contrary, DASMC were initially perfused with hypoxic PSS for 25 min, and then randomly changed to normoxia or kept in hypoxia for the last 5 min. Thereafter, cells were immediately fixed with 4% paraformaldehyde, washed with phosphate-buffered saline (PBS) and permeabilized with 0.4% Triton and 3% bovine serum albumin bovine for 1 h. Cells were incubated with 1:30 dilution of mouse anticeramide antibody at 4°C over-night, and then for 15 min at 37°C. Coverslips were washed with blocking buffer and exposed to FITC-conjugated anti-mouse secondary antibody for 2 h a 37°C. After washing, immunofluorescent signals were viewed using an inverted non-confocal fluorescent microscope. Fluorescence was quantified using ImageJ (ver 1.32j, NIH, http://rsb.info.nih/ij/). Intensity values were normalized by cell surface after subtracting background. For each condition, a minimum of four coverslips from at least three separate samples (derived from different animals) were used for quantification. Pictures were taken and analyzed by a blind observer, unaware of the treatment. In selected experiments, PASMCs exposed to hypoxic PSS were assessed for the presence of ceramide in the outer leaflet of the plasma membrane by removing the permeabilization step from the immunofluorescence labeling process. These preparations were examined with a confocal laser scanning fluorescent microscope (Centro de Microscopía, Universidad Complutense de Madrid).

Determination of ROS

The fluorescent dye DCF was used to asses ROS production. Although this dye is far the commonest probe used to detect ROS, it can be oxidized by other free radicals (50). Thus, measurements were compared with parallel time controls, positive controls (t-butylhydroperoxide) and experiments in the presence of ROS generating system inhibitors. Endothelium denuded PA and pDA segments were incubated with the membrane-permeable diacetate form of DCF (DCF-DA, 10 μM) for 60–90 min. Vessels were then placed in the stage of a fluorescent inverted microscope (Leica DM IRB), superfused with PSS (2 ml/min). Preparations were allowed to equilibrate for 30 min under normoxic (for PA) or hypoxic (for DA) conditions, in the absence or in the presence of VAS2870, apocynin or rotenone. Finally, vessels were illuminated through the luminal surface using a 450–490 nm band-pass filter. The emitted fluorescence was filtered using 515 nm long-pass emission filter. Images were taken at 1 min intervals with a Leica DC300F color digital camera. Fluorescence was quantified using ImageJ. Intensity values are reported as a percent of the initial values after subtracting background. After fluorescence values were stable, preparations were challenged with a hypoxic (for PA) or a normoxic (for DA) solution in the continuous absence or presence of apocynin or VAS2870.

RT-PCR analysis

Total RNA was isolated and purified from PA, CA, aDA, and pDA homogenates using RNeasy Fibrous Tissue Mini kit (Qiagen). Total RNA was reverse transcribed into cDNA using iScript™ cDNA Synthesis Kit (BioRad) following manufacturer's instructions. RT-PCR was performed using a Taqman system (Roche-Applied Biosystems) in the Unidad de Genómica (Universidad Complutense de Madrid). Specific primers were designed for the chicken nSMase gene *SMPD3*.

Lipid extraction and ceramide species measurement

Quantitative evaluation of the proportion of ceramide to the main PC (34:2) was performed by UHPLC-MS. Samples were thawed and 100 μl ethanol added to every tube and vortex-mixed for 5 min. The suspensions were transferred into 0.5 ml microcentrifuge tubes where 5–10 μg of glass beads (acid-washed, 150–212 μm; Sigma-Aldrich) had been prepared. Lipids were then extracted by vigorous shaking with a TissueLyser LT from Qiagen for 15 min, at 50 rpm. Tubes were further centrifuged at 15400 g and 15°C for 20 min, and 80 μl from the supernatant was transferred to HPLC vials with insert. The samples were analyzed with an UHPLC-QTOF MS from Agilent Technologies, equipped with a 1290 series LC system and a 6550 iFunnel QTOF MS detector. About 0.5 μl from each sample was injected (in triplicate) onto the column, a Zorbax Eclipse Plus C8, 2.1 × 150 mm; 1.8 μm (Agilent Technologies) kept at 80°C. Compounds were eluted with an 8 min linear gradient for the mobile phase at 0.6 ml/min, from 50% ammonium formate 10 mM (pH 6.6) and 50% methanol to 100% methanol. Data files were processed with MassHunter Qualitative Analysis B.05.00 to clean of background noises and unrelated ions by the Molecular Feature Extraction tool. Data pretreatment, including alignment and filtering was performed in MassProfiler Professional (B.12.01; Agilent Technologies). The result was a matrix with all the compounds in the samples sorted by their characteristic retention time and neutral mass, and the abundance of each compound for each sample. The list of exact masses was exported to public databases (METLIN—http://metlin.scripps.edu/; LipidMaps—www.lipidmaps.org/; and KEGG—www.genome.jp/kegg/), and the features for ceramides and PC (34:2) were identified by the exact mass (less than 5 ppm error).

Electrophysiological studies

Membrane currents were recorded with an Axopatch 200B and a Digidata 1322A (Axon Instruments) using the whole-cell configuration of the patch clamp technique. Currents were evoked by applying depolarizing steps, normalized for cell capacitance and expressed in pA/pF as previously described (10, 11). Current-voltage relationships were constructed by measuring the currents at the end of the pulse. For recording optimal Kv currents, cells were superfused with an external Ca^{2+}-free PSS (see above) and a Ca^{2+}-free pipette (internal) solution containing (mM): KCl 110, $MgCl_2$ 1.2, Na_2ATP 5, HEPES 10, EGTA 10, pH adjusted to 7.3 with KOH. All experiments were performed at room temperature (22°C

– 24°C). Experiments were performed under normoxic or hypoxic conditions for PASMC or DASMC, respectively.

Data analysis

Data are expressed as means ± SEM; *n* indicates the number of samples from different animals or patients. For multiple comparisons, statistical analysis was performed using a one or two way ANOVA followed by a Bonferroni *post hoc* test, otherwise using a two-tailed Student's *t*-test for paired or unpaired observations. Differences were considered statistically significant when $p < 0.05$.

Acknowledgments

This work was supported by the Spanish Ministerio de Ciencia e Innovación (predoctoral FPI grant to D.M-C.; research grants SAF2010-22066-C02-02 to A.C.; SAF2008-03948 and SAF2011-28150 to F.P.V.; SAF2011-26443 to J.C.; Juan de la Cierva contract to L.M.), the Spanish Ministry of Education (predoctoral FPU grant to J.M.-S.), Spanish Ministry of Economy and Competitiveness (research grant CTQ2011-23562 to F.J.R.), and Marie Curie European Reintegration Grant within the 7th European Community Framework Programme (PERG05-GA-2009-249165 to F.P.V. and L.M.). A.F. was funded from the European Union 7th Framework Programme (FP7/2007–2013) under grant agreement no. 264864. The authors thank Dr. Coral Barbas for her generous support and advice for the determination of ceramides.

Author Disclosure Statement

No competing financial interests exist

References

1. Agren P, Cogolludo AL, Kessels CG, Perez-Vizcaino F, De Mey JG, Blanco CE, and Villamor E. Ontogeny of chicken ductus arteriosus response to oxygen and vasoconstrictors. *Am J Physiol Regul Integr Comp Physiol* 292: R485–R496, 2007.
2. Archer SL, Souil E, Dinh-Xuan AT, Schremmer B, Mercier JC, El Yaagoubi A, Nguyen-Huu L, Reeve HL, and Hampl V. Molecular identification of the role of voltage-gated K+ channels, Kv1.5 and Kv2.1, in hypoxic pulmonary vasoconstriction and control of resting membrane potential in rat pulmonary artery myocytes. *J Clin Invest* 101: 2319–2330, 1998.
3. Bai J and Pagano RE. Measurement of spontaneous transfer and transbilayer movement of BODIPY-labeled lipids in lipid vesicles. *Biochemistry* 36: 8840–8848, 1997.
4. Belanger C, Copeland J, Muirhead D, Heinz D, and Dzialowski EM. Morphological changes in the chicken ductus arteriosi during closure at hatching. *Anat Rec (Hoboken)* 291: 1007–1015, 2008.
5. Bourbon NA, Yun J, and Kester M. Ceramide directly activates protein kinase C zeta to regulate a stress-activated protein kinase signaling complex. *J Biol Chem* 275: 35617–35623, 2000.
6. Chadha PS, Zunke F, Zhu HL, Davis AJ, Jepps TA, Olesen SP, Cole WC, Moffatt JD, and Greenwood IA. Reduced KCNQ4-encoded voltage-dependent potassium channel activity underlies impaired *β*-adrenoceptor-mediated relaxation of renal arteries in hypertension. *Hypertension* 59: 877–884, 2012.
7. Cogolludo A, Moral-Sanz J, van der Sterren S, Frazziano G, van Cleef A, Menendez C, Zoer B, Moreno E, Roman A, Perez-Vizcaino F, and Villamor E. Maturation of O-2 sensing and signaling in the chicken ductus arteriosus. *Am J Physiol Lung Cell Mol Physiol* 297: L619–L630, 2009.
8. Cogolludo A, Moreno L, Frazziano G, Moral-Sanz J, Menendez C, Castaneda J, Gonzalez C, Villamor E, and Perez-Vizcaino F. Activation of neutral sphingomyelinase is involved in acute hypoxic pulmonary vasoconstriction. *Cardiovasc Res* 82: 296–302, 2009.
9. This reference has been deleted.
10. Cogolludo A, Moreno L, Lodi F, Frazziano G, Cobeno L, Tamargo J, and Perez-Vizcaino F. Serotonin inhibits voltage-gated K+ currents in pulmonary artery smooth muscle cells – Role of 5-HT2A receptors, caveolin-1, and K(V)1.5 channel internalization. *Circ Res* 98: 931–938, 2006.
11. Cogolludo AL, Moral-Sanz J, van der Sterren S, Frazziano G, van Cleef AN, Menendez C, Zoer B, Moreno E, Roman A, Perez-Vizcaino F, and Villamor E. Maturation of O2 sensing and signaling in the chicken ductus arteriosus. *Am J Physiol Lung Cell Mol Physiol* 297: L619–L630, 2009.
12. Contreras FX, Sánchez-Magraner L, Alonso A, and Goñi FM. Transbilayer (flip-flop) lipid motion and lipid scrambling in membranes. *FEBS Lett* 584: 1779–1786, 2010.
13. Dzialowski EM, Sirsat T, van der Sterren S, and Villamor E. Prenatal cardiovascular shunts in amniotic vertebrates. *Respir Physiol Neurobiol* 178: 66–74, 2011.
14. Frazziano G, Moreno L, Moral-Sanz J, Menendez C, Escolano L, Gonzalez C, Villamor E, Alvarez-Sala JL, Cogolludo AL, and Perez-Vizcaino F. Neutral sphingomyelinase, NADPH oxidase and reactive oxygen species. Role in acute hypoxic pulmonary vasoconstriction. *J Cell Physiol* 226: 2633–2640, 2011.
15. Gao Y and Raj JU. Regulation of the pulmonary circulation in the fetus and newborn. *Physiol Rev* 90: 1291–1335, 2010.
16. Gonzalez C, Agapito MT, Rocher A, Gomez-Nino A, Rigual R, Castaneda J, Conde SV, and Obeso A. A revisit to O2 sensing and transduction in the carotid body chemoreceptors in the context of reactive oxygen species biology. *Respir Physiol Neurobiol* 174: 317–330, 2011.
17. Greyner H and Dzialowski EM. Mechanisms mediating the oxygen-induced vasoreactivity of the ductus arteriosus in the chicken embryo. *Am J Physiol Regul Integr Comp Physiol* 295: R1647–R1659, 2008.
18. Gulbins E and Li PL. Physiological and pathophysiological aspects of ceramide. *Am J Physiol Regul Integr Comp Physiol* 290: R11–R26, 2006.
19. Hajduch E, Turban S, Le Liepvre X, Le Lay S, Lipina C, Dimopoulos N, Dugail I, and Hundal HS. Targeting of PKCzeta and PKB to caveolin-enriched microdomains represents a crucial step underpinning the disruption in PKB-directed signalling by ceramide. *Biochem J* 410: 369–379, 2008.
20. Hampl V, Bibova J, Stranak Z, Wu X, Michelakis ED, Hashimoto K, and Archer SL. Hypoxic fetoplacental vasoconstriction in humans is mediated by potassium channel inhibition. *Am J Physiol Heart Circ Physiol* 283: H2440–H2449, 2002.
21. Hampl V and Jakoubek V. Regulation of fetoplacental vascular bed by hypoxia. *Physiol Res* 58 Suppl 2: S87–S93, 2009.
22. Hong Z, Hong F, Olschewski A, Cabrera JA, Varghese A, Nelson DP, and Weir EK. Role of store-operated calcium channels and calcium sensitization in normoxic contraction of the ductus arteriosus. *Circulation* 114: 1372–1379, 2006.

23. Howard RB, Hosokawa T, and Maguire MH. Hypoxia-induced fetoplacental vasoconstriction in perfused human placental cotyledons. *Am J Obstet Gynecol* 157: 1261–1266, 1987.
24. Jabr RI, Toland H, Gelband CH, Wang XX, and Hume JR. Prominent role of intracellular Ca2+ release in hypoxic vasoconstriction of canine pulmonary artery. *Br J Pharmacol* 122: 21–30, 1997.
25. Jakoubek V, Bibova J, and Hampl V. Voltage-gated calcium channels mediate hypoxic vasoconstriction in the human placenta. *Placenta* 27: 1030–1033, 2006.
26. Kajimoto H, Hashimoto K, Bonnet SN, Haromy A, Harry G, Moudgil R, Nakanishi T, Rebeyka I, Thebaud B, Michelakis ED, and Archer SL. Oxygen activates the Rho/Rho-kinase pathway and induces RhoB and ROCK-1 expression in human and rabbit ductus arteriosus by increasing mitochondria-derived reactive oxygen species: a newly recognized mechanism for sustaining ductal constriction. *Circulation* 115: 1777–1788, 2007.
27. Keck M, Resnik E, Linden B, Anderson F, Sukovich DJ, Herron J, and Cornfield DN. Oxygen increases ductus arteriosus smooth muscle cytosolic calcium via release of calcium from inositol triphosphate-sensitive stores. *Am J Physiol Lung Cell Mol Physiol* 288: L917–L923, 2005.
28. Lindgren I, Zoer B, Altimiras J, and Villamor E. Reactivity of chicken chorioallantoic arteries, avian homologue of human fetoplacental arteries. *J Physiol Pharmacol* 61: 619–628, 2010.
29. Liu B Andrieu-Abadie N, Levade T, Zhang P, Obeid LM, and Hannun YA. Glutathione regulation of neutral sphingomyelinase in tumor necrosis factor-alpha-induced cell death. *J Biol Chem* 273: 11313–11320, 1998.
30. Lu W, Wang J, Peng G, Shimoda LA, and Sylvester JT. Knockdown of stromal interaction molecule 1 attenuates store-operated Ca2+ entry and Ca2+ responses to acute hypoxia in pulmonary arterial smooth muscle. *Am J Physiol Lung Cell Mol Physiol* 297: L17–L25, 2009.
31. López-Montero I, Rodriguez N, Cribier S, Pohl A, Vélez M, and Devaux PF. Rapid transbilayer movement of ceramides in phospholipid vesicles and in human erythrocytes. *J Biol Chem* 280: 25811–25819, 2005.
32. McMurtry IF, Davidson AB, Reeves JT, and Grover RF. Inhibition of hypoxic pulmonary vasoconstriction by calcium antagonists in isolated rat lungs. *Circ Res* 38: 99–104, 1976.
33. Michelakis E, Rebeyka I, Bateson J, Olley P, Puttagunta L, and Archer S. Voltage-gated potassium channels in human ductus arteriosus. *Lancet* 356: 134–137, 2000.
34. Michelakis ED, Rebeyka I, Wu X, Nsair A, Thebaud B, Hashimoto K, Dyck JR, Haromy A, Harry G, Barr A, and Archer SL. O2 sensing in the human ductus arteriosus: regulation of voltage-gated K+ channels in smooth muscle cells by a mitochondrial redox sensor. *Circ Res* 91: 478–486, 2002.
35. Mittal M, Gu XQ, Pak O, Pamenter ME, Haag D, Fuchs DB, Schermuly RT, Ghofrani HA, Brandes RP, Seeger W, Grimminger F, Haddad GG, and Weissmann N. Hypoxia induces Kv channel current inhibition by increased NADPH oxidase-derived reactive oxygen species. *Free Radic Biol Med* 52: 1033–1042, 2012.
36. Moral-Sanz J, Gonzalez T, Menendez C, David M, Moreno L, Macias A, Cortijo J, Valenzuela C, Perez-Vizcaino F, and Cogolludo A. Ceramide inhibits Kv currents and contributes to TP-receptor-induced vasoconstriction in rat and human pulmonary arteries. *Am J Physiol Cell Physiol* 301: C186–C194, 2011.
37. Morio Y and McMurtry IF. Ca(2+) release from ryanodine-sensitive store contributes to mechanism of hypoxic vasoconstriction in rat lungs. *J Appl Physiol* 92: 527–534, 2002.
38. Olschewski A, Hong Z, Peterson DA, Nelson DP, Porter VA, and Weir EK. Opposite effects of redox status on membrane potential, cytosolic calcium, and tone in pulmonary arteries and ductus arteriosus. *Am J Physiol Lung Cell Mol Physiol* 286: L15–L22, 2004.
39. Perez-Vizcaino F, Cogolludo A, and Moreno L. Reactive oxygen species signaling in pulmonary vascular smooth muscle. *Respir Physiol Neurobiol* 174: 212–220, 2010.
40. Ramstrom C, Chapman H, Ekokoski E, Tuominen RK, Pasternack M, and Tornquist K. Tumor necrosis factor alpha and ceramide depolarise the resting membrane potential of thyroid FRTL-5 cells via a protein kinase Czeta-dependent regulation of K+ channels. *Cell Signal* 16: 1417–1424, 2004.
41. Rathore R, Zheng YM, Niu CF, Liu QH, Korde A, Ho YS, and Wang YX. Hypoxia activates NADPH oxidase to increase [ROS]i and [Ca2+]i through the mitochondrial ROS-PKCepsilon signaling axis in pulmonary artery smooth muscle cells. *Free Radic Biol Med* 45: 1223–1231, 2008.
42. Reeve HL, Tolarova S, Nelson DP, Archer S, and Weir EK. Redox control of oxygen sensing in the rabbit ductus arteriosus. *J Physiol* 533: 253–261, 2001.
43. Robertson TP, Dipp M, Ward JP, Aaronson PI, and Evans AM. Inhibition of sustained hypoxic vasoconstriction by Y-27632 in isolated intrapulmonary arteries and perfused lung of the rat. *Br J Pharmacol* 131: 5–9, 2000.
44. Robertson TP, Hague D, Aaronson PI, and Ward JP. Voltage-independent calcium entry in hypoxic pulmonary vasoconstriction of intrapulmonary arteries of the rat. *J Physiol* 525 Pt 3: 669–680, 2000.
45. Smith GC. The pharmacology of the ductus arteriosus. *Pharmacol Rev* 50: 35–58, 1998.
46. Sylvester JT, Shimoda LA, Aaronson PI, and Ward JP. Hypoxic pulmonary vasoconstriction. *Physiol Rev* 92: 367–520, 2012.
47. Tristani-Firouzi M, Reeve HL, Tolarova S, Weir EK, and Archer SL. Oxygen-induced constriction of rabbit ductus arteriosus occurs via inhibition of a 4-aminopyridine-, voltage-sensitive potassium channel. *J Clin Invest* 98: 1959–1965, 1996.
48. Ward JP. Oxygen sensors in context. *Biochim Biophys Acta* 1777: 1–14, 2008.
49. Ward JP and McMurtry IF. Mechanisms of hypoxic pulmonary vasoconstriction and their roles in pulmonary hypertension: new findings for an old problem. *Curr Opin Pharmacol* 9: 287–296, 2009.
50. Wardman P. Fluorescent and luminescent probes for measurement of oxidative and nitrosative species in cells and tissues: progress, pitfalls, and prospects. *Free Radic Biol Med* 43: 995–1022, 2007.
51. Waypa GB, Guzy R, Mungai PT, Mack MM, Marks JD, Roe MW, and Schumacker PT. Increases in mitochondrial reactive oxygen species trigger hypoxia-induced calcium responses in pulmonary artery smooth muscle cells. *Circ Res* 99: 970–978, 2006.
52. Waypa GB and Schumacker PT. Hypoxia-induced changes in pulmonary and systemic vascular resistance: where is the O2 sensor? *Respir Physiol Neurobiol* 174: 201–211, 2010.
53. Weir EK and Archer SL. The mechanism of acute hypoxic pulmonary vasoconstriction: the tale of two channels. *FASEB J* 9: 183–189, 1995.
54. Weir EK and Archer SL. The role of redox changes in oxygen sensing. *Respir Physiol Neurobiol* 174: 182–191, 2010.

55. Weir EK, Lopez-Barneo J, Buckler KJ, and Archer SL. Acute oxygen-sensing mechanisms. *N Engl J Med* 353: 2042–2055, 2005.
56. Yuan XJ, Goldman WF, Tod ML, Rubin LJ, and Blaustein MP. Hypoxia reduces potassium currents in cultured rat pulmonary but not mesenteric arterial myocytes. *Am J Physiol* 264: L116–L123, 1993.
57. Yuan XJ, Tod ML, Rubin LJ, and Blaustein MP. Deoxyglucose and reduced glutathione mimic effects of hypoxia on K+ and Ca2+ conductances in pulmonary artery cells. *Am J Physiol* 267: L52–L63, 1994.
58. Zoer B, Kessels L, Vereijken A, De Mey JG, Bruggeman V, Decuypere E, Blanco CE, and Villamor E. Effects of prenatal hypoxia on pulmonary vascular reactivity in chickens prone to pulmonary hypertension. *J Physiol Pharmacol* 60: 119–130, 2009.

Address correspondence to:
Dr. Angel Cogolludo
Department of Pharmacology
School of Medicine
Universidad Complutense Madrid
Ciudad Universitaria S/N 28040 Madrid
Spain

E-mail: acogolludo@med.ucm.es

Date of first submission to ARS Central, June 12, 2012; date of final revised submission, June 2, 2013; date of acceptance, June 2, 2013.

Abbreviations Used

4-AP = 4-aminopyridine
aDA = aortic side of the ductus arteriosus
CA = chorioallantoic arteries
DA = ductus arteriosus
DASMC = ductus arteriosus smooth muscle cells
DCF = 2,7-dichlorofluorescein
ET-1 = endothelin-1
HPV = hypoxic pulmonary vasoconstriction
Kv = voltage-gated potassium
nSMase = neutral sphingomyelinase
PA = pulmonary arteries
PASMC = pulmonary artery smooth muscle cells
PBS = phosphate-buffered saline
PC = phosphatidylcholine
pDA = pulmonary side of the ductus arteriosus
PKC = protein kinase C
PKCζ-PI = PKCζ peptide inhibitor
PSS = physiological salt solution
ROS = reactive oxygen species
RT-PCR = real-time–polymerase chain reaction
SMase = sphingomyelinase
SNP = sodium nitroprusside
TBH = t-butylhydroperoxide
UHPLC-MS = ultra high performance liquid chromatography–mass spectrometry